Publishing House
AKAPIT

COMPUTER METHODS IN MATERIALS SCIENCE

Informatyka w Technologii Materiałów

Vol. 10, 2010, No. 3

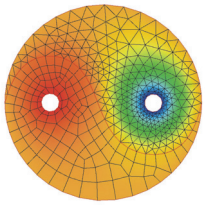

THE NUMERICAL ANALYSIS OF RIVET DEFORMATION WHEN JOINING ALUMINUM SHEETS USING SELF-PIERCE RIVETING METHOD

JACEK MUCHA

Rzeszow University of Technology, ul. Wincentego Pola 2, 35-959 Rzeszów, Poland
j_mucha@prz.edu.pl

Abstract

Self-piercing riveting (SPR) is becoming an important joining technique for the automotive applications of aluminum sheets. SPR is essentially a cold forming process, in which a semi-tubular rivet, pressed by a plunger, pierces through the thickness of the upper sheet and flares into the bottom sheet, forming a mechanical interlock between the two sheets.

In this paper, the riveting process has been simulated numerically using the finite element code MSC Marc. The results show the capability to simulate the riveting process for different combination of rivet material and the joined sheet pressure conditions. The riveting analysis has been performed for joined aluminum sheets. Based on the numerical calculation results, the author explains the riveting process phenomena. The comparison analysis has been performed within the numerical experiment range to cover the effect of various riveting process parameters on the rivet deformation.

Key words: finite element modelling, joint formation, self-pierce riveting, modeling of process

NOMENCLATURE

E	Young's modulus
σ_{02}^{r}	true stress at 0.2% plastic strain - rivet
σ_{02}^{s}	true stress at 0.2% plastic strain - sheets
S_σ	sheet and rivet yield point index
σ_p	flow stress
ε	true plastic strain
K	strain hardening curve coefficient
n	strain hardening curve exponent
δ_t	upper to lower sheet thickness ratio index
t_{st}	thickness top sheets
t_{sb}	thickness bottom sheets
D_{rmin}	minimum diameter of tubular rivet part in joint
D_{rmax}	maximum diameter of tubular rivet part in joint
S_{Dr}	rivet spread index
h_1	joint height on lower sheet
h_2	rivet head surface offset under upper sheet surface
h_3	rivet head surface protruding above upper sheet surface
s	punch displacement

1. INTRODUCTION

Self Piercing Riveting (SPR) is a cold forming process used to join two or three layers of material by driving a rivet through the top layers of material and upsetting the rivet in the lower layer without piercing the lower material. SPR technology is a relatively new fastening technique that enables to join such different metals. The effectiveness of SPR joining, compared to other cold joining methods, is satisfactory (Di Lorenzo & Landolfo, 2004). SPR is widely used when manufacturing aluminum bodyworks of modern vehicles, as presented among the others by Barnes and Pashby (2000) and Cai et al. (2005).

Unlike conventional riveting, self-piercing riveting does not require a pre-drilled hole, because the rivet makes its own hole as it is being inserted. This brings great benefits in terms of production cost reduction and ease of use compared to conventional

ISSN 1641-8581

riveting. The increasing use of coated, lightweight and high-strength materials, such as galvanized or pre-painted steel and aluminium has led industries to re-examine traditional methods of assembling components. As welding of these materials is difficult or impossible, and assembly using conventional rivets is slow and costly, the benefits of a process that combines high joint integrity with rapid assembly times become obvious. The detailed characteristics of such a new joining technology has been presented by Mucha (2007).

A thorough study of the self-pierce riveting process was done by Hahn and Dölle (2001). An experimental test rig was established that enables to measured force during the riveting process. Moreover, a numerical model of the riveting process was made using the finite element (FE) program MSC.AutoForge. Here, a geometric failure criterion on the minimum allowable sheet thickness was used to predict failure in the numerical model.

Atzeni et al. (2003, 2004, 2009), dealt systematically with numerical and experimental investigations of SPR joints, producing detailed suggestions for the numerical modelling of SPR process parameters such as friction coefficients of the different interfaces. A basic FE model of the indentation of an SPR process was created and analysed using Deform-2D (Gårdstam, 2006). This enabled initial calculations of the setting forces, displacements and component deformations to be compared with that of actual fastenings. The numeric simulation of the SPR process was extensively covered by Cacko and Czyżewski (2004, 2007) in which a numerical model of the SPR process was made using the FE programme MSC.Marc and MSC.SuperForm MSC.AutoForge. The objective of this study is to present and discuss the possibility to simulate the riveting process using the commercial finite element code LS-Dyna (Porcaro et al., 2006). Atzeni et al. (2009) developed lightweight self-piercing riveting equipment using FE meshes. These were generated using field analysis modeller (FAM) and analysed using the general purpose FE code ABAQUS. The analysis of effects, occurring during the self piercing riveting, based on MSC. Marc numerical calculations has been presented by Mucha (2009a).

The numerical simulation results enable better understanding the effects, occurring when creating the SPR joint. The selected aspects of SPR joining technology design based on FEM simulation using MSC. Marc have been presented by Mucha (2009b). Very interesting paper, from the joining process numerical modeling point of view (using Forge2005 software), has been presented by Bouchard et al. (2009).

However, the numerical analysis of the rivet deformation for various riveting parameters has not been presented in any paper. This paper presents the results of the self-pierce riveting process analysis and the rivet deformation during the process. The numerical FEM simulation results may be used when designing those modern joints both for other arrangements of joined sheet mechanical properties and the technology used to create them.

2. JOINT CREATION PROCESS

The self-piercing rivet is squeezed at high force into the material to be joined, piercing the top sheets of material and spreading outwards into the bottom sheet of material, under the influence of an upsetting die, to form a strong joint. The rivet setting tool is powered hydraulically from a separate power pack, which also controls the tool sequencing. Rivets are fed automatically into the setting tool on a plastic belt, thus allowing automated, high volume production. In figure 1 there is another description of the rivet setting process. The riveting machine is supplied with rivets from the belt magazine (figure 1b) or individual rivets are taken from the magazine of pneumatic feeder. The rivet overview is presented on figure 1c.

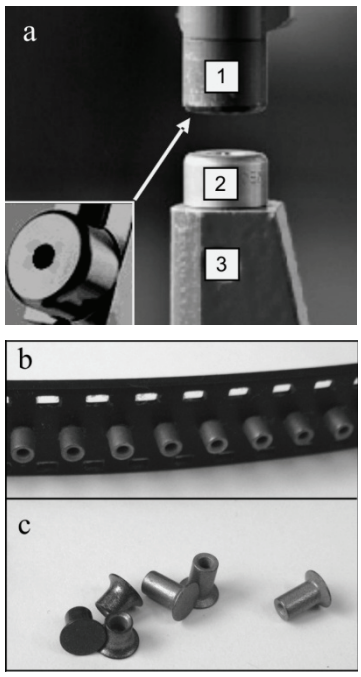

Fig. 1. *Partial view: a) of real world SPR riveting machine (1 – blank-holder, 2 – die, 3 – mounting), b) belt magazine with rivets, c) individual rivets (supplied to the magazine of the pneumatic feeder).*

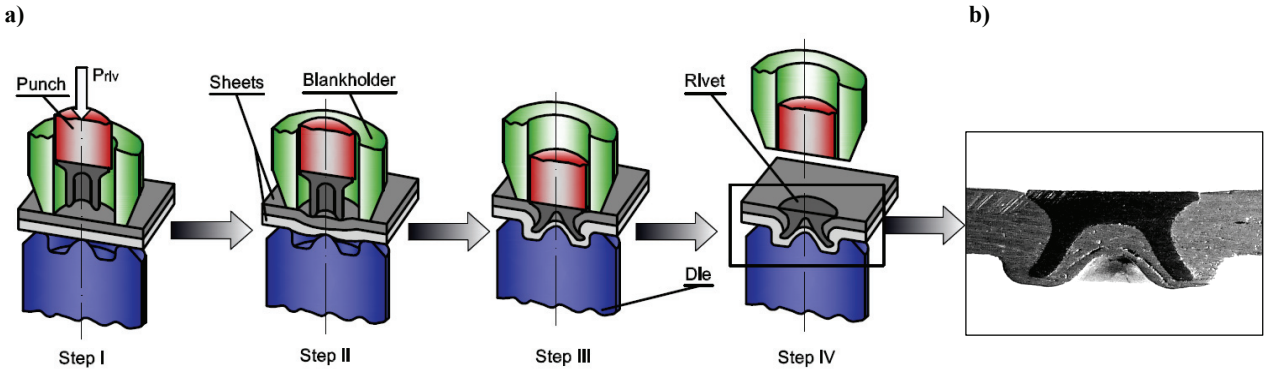

Fig. 2. Self-piercing riveting process: a) *schematic representation of the SPR, b) cross-section.*

The self-piercing riveting process can be described by the following four steps (see figure 2a):

- clamping (step I), the blank-holder presses the two sheets against the die, and now the rivet is gradually pressed into aluminum sheets;
- piercing (step II), the punch pushes the rivet into the top plate;
- flaring (step III), the material of the lower sheet flows into the die and the rivet shank begins to flare outward, forming a mechanical interlock between the upper and lower substrates;
- release of the punch (IV step), finally, once the punch is retracted, the finished joint is achieved with the fastener properly seated in the sheets.

The cross section of a typical joint after riveting is shown in figure 2b.

2. NUMERICAL EXPERIMENT

Self rivet installation is a new technology. It does not require a hole before the installation. The rivet penetrates the plate and forms a joint in one operation.

Rivet installation is often used to assemble two or more plates. Self rivet installation depends on the deformation of the rivet and penetration of the plates which can be predicted by the simulation. The loading required for the installation can also be predicted.

The complex state of stress, existing in the finished riveted joint, leads the detailed analysis of effects in such joints to the solving of the physically and geometrically non-linear mechanical issue. The numerical computations have been performed in MSC Marc Mentat 2005 software, where an additional procedure enabling the material separation has been applied.

Due to a form of the joint itself and the course of forming, the self piercing riveting process may be considered using the two-dimensional axisymmetric model - the axisymmetric state of stress and strains. A 2D axisymmetric model of the riveting process was generated including two sheets to be joined, the rivet and the tools. The boundary conditions have been defined based on the SPR riveting (figure 4). When modeling the basic die and rivet form, the corresponding geometry parameters of *Böllhoff* tooling have been used. The die with a corresponding impression has been placed in a mounting of the riveting machine (the mounting is defined as a rigid bearing surfaces for a die), and the upper and lower aluminum sheets are placed on a die, where the lower sheet continuously contacts the die surface - see figure 3. The blank-holder continuously contacts the upper sheet until completion of the riveting process; then the blank-holder returns to its home position.

Firstly, a displacement is prescribed for the blankholder. When the sheets are clamped between the blankholder and the die, a pressure is applied to the blankholder in order to keep the sheets tight. Secondly, a displacement is prescribed for the punch that pushes the rivet through the sheets until the joint is formed.

The blank-holder displacement, required for such a die form, is assumed in order to perform an initial sheet bending, and its value equals the offset of the conical part above its front surface - 0.5 mm. The punch displacement has been established so that the punch moves a distance to flush the front surface of a rivet with the an upper sheet surface (s_{max}).

The sheets being joined and the rivet have been modeled using the elastic-plastic material model with an isotropic hardening, using the quadrilateral axisymmetric element of type 10. As the problem is axisymmetric, the four-node 2D axisymmetric elements have been used, with four Gauss points. The joined sheet plates are subject to huge local plastic strains when the SPR joint is being created. The mesh rendering algorithm was used in order to achieve correct and stable numerical calculations.

The maximum allowed element length of 0,2 mm was taken as a parameter. Such defined parameters of mesh reconstruction enabled stable solving of issue in each computation step. The upper sheet material thickness, where the mesh elements were split at their contact boundary, was set as 0,02 mm. At the end of each computation step the routine checks whether the distance between two nodes on the boundary of selected material is not lower than the user defined distance. If the condition is met, two adjacent elements, for which the critical distance was observed, are split along the common edge.

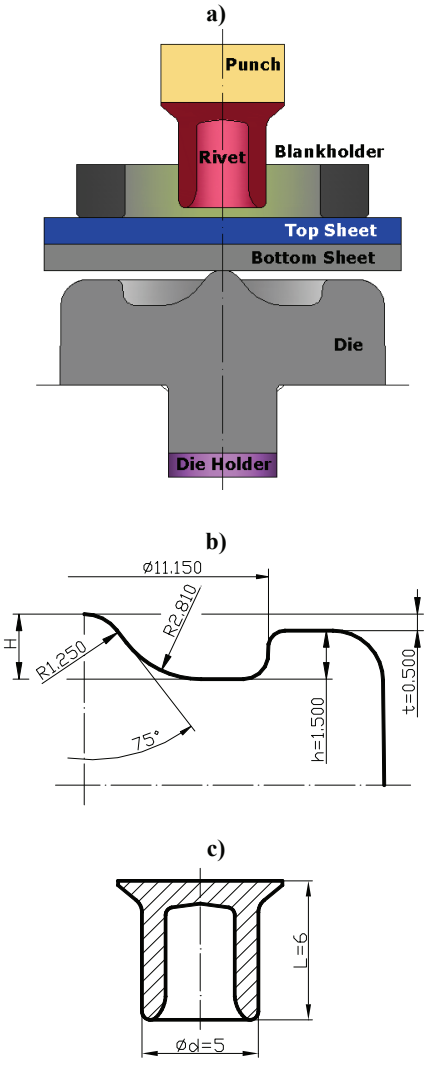

Fig. 3. *Schematic representation of the numerical model – a) and the die geometry –b), rivet geometry – c).*

The rivet is made of boron steel, and the sheets are aluminium alloy. The numerical experiment has been limited to the sheets of identical material: Al/Al. The mechanical properties of the rivet and sheets are shown in table 1. For joining purposes, the upper to lower sheet thickness ratio (1) of 1mm/2mm in form of an indicator (1) has been assumed:

$$\delta_t = \frac{t_{st}}{t_{sb}}. \tag{1}$$

The rivet has enough hardness to piece the sheets, whereas the rivet is plastically deformed and the tubular leg of the rivet spreads. The flow stress of the rivet and sheets are obtained from the uniaxial compression and tensile tests, respectively, and the flow stress is used in the simulation. The material hardening effect has been described by the $\sigma = f(\varepsilon)$ relationship, using the Hollomon's equation (2):

$$\sigma_p = K \cdot \varepsilon^n. \tag{2}$$

Table 1. *Mechanical properties for rivet and sheets.*

Material		E [GPa]	$\sigma_{0.2}$ [MPa]	Material model	Flow stress	
					K [MPa]	n
Rivet	Boron steel	188	1520	1	2627	0.088
			1176	2	1970	
			980	3	1642	
			1520	4	1659	0.014
Sheets	Aluminium alloy	75	135	505		0.191

The joined sheet and rivet yield point ratio (3) significantly influences the joint creation process:

$$S_\sigma = \frac{\sigma_{02}^r}{\sigma_{02}^s}, \tag{3}$$

so this relationship has been additionally designated as S_σ. For the examined material models 1, 2, 3, 4, the S_σ values have been respectively: 11.26, 8.71, 7.26.

Note that the difference of yield stresses for upper and lower sheet affects also the joint part behavior when pressing the rivet.

3. RESULTS OF THE NUMERICAL SYMULATION

The die with a conical impression in its middle part (with an offset of 0.5 mm from a sheet pressure surface) has been used for the purpose of a simulation, and the joined elements, mainly the lower sheet, has rested on the conical part of a die (figure 3). When executing the joining process, in the first stage of riveting, the sheets being joined are pressed to the die surface by the blank-holder. This resulted in an initial strain of the elements being joined. And

now the rivet is gradually pressed into aluminum sheets.

Pressing the fastener into sheets causes that the elastic strains continuously increase, and in turn the yield point is achieved and exceeded both for the rivet, and the sheets being joined. It is important that the rivet material plastifying has to occur much more later than for elements being joined. The plastifying role is to form the sheets in the die impression, and then the first sheet is punctured. The elastic strains exist on the rivet until the upper sheet material is separated. The highest strains exist in the tubular part (figure 4) and equal 1380 MPa. Further rivet pressing causes its spreading towards outside. The course of tubular river part diameter increase may be observed by giving the displacement values of the points on the rivet (I, II – see figure 5), as presented on the corresponding curves on figure 6.

The rivet response to specified boundary conditions of the process is e.g. its spreading course, which may be characterized by the course of its corresponding diameter ratio (4):

$$S_{Dr} = \frac{D_{r_{\max}}}{D_{r_{\min}}}. \qquad (4)$$

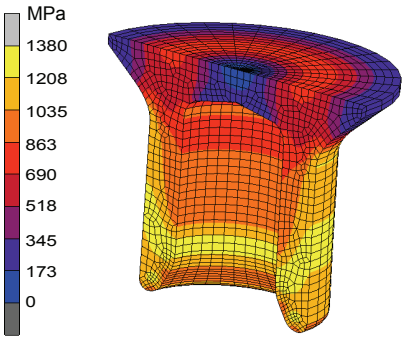

Fig. 4. *Equivalent stress distribution in the rivet by HMH (separation of the upper sheet).*

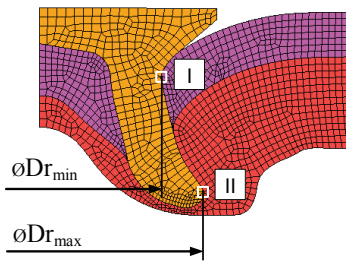

Fig. 5. *Numerical model of joint with the measurement points on the rivet: I and II.*

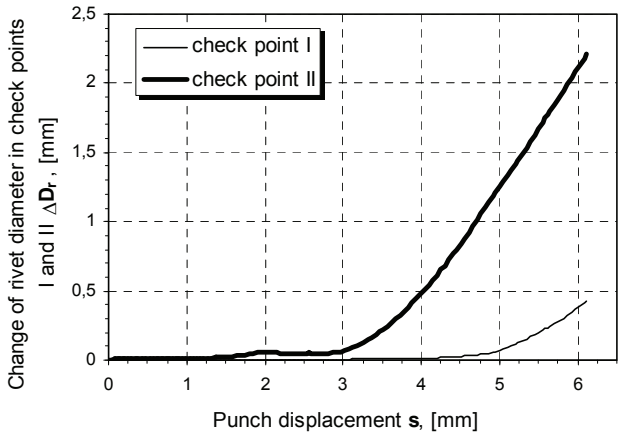

Fig. 6. *The rivet tubular part diameter change curves in specified points during the joint forming process (point displacements in y direction of numerical model vs. punch displacement).*

When the conically shaped die is used, the riveted joint of thin aluminum sheets has a specific form on the second sheet side in form of a "flash". Joined this way thin-walled elements are finally subjected to specific deformations and plastic strains within the joint area. Then the high plastic strains of the joint elements exist, and these plastic strains achieve a maximum value - see figure 7 and 8. Due to different levels of strains for individual joint elements, the author has decided to present the finished joint and the rivet separately. This enabled more clear emphasizing their material strain in form of specific field distributions. The highest strain level may be observed in the upper sheet (the area "1" on figure 7) due to its material cohesion loss. Slightly lower level exists in the lower sheet from inside - its contact surface with the die (area "2" on figure 7). The maximum plastic strain areas in the river are placed close to the end of its tubular part (figure 8) - outside it is an area "1", and inside it is: an area "2".

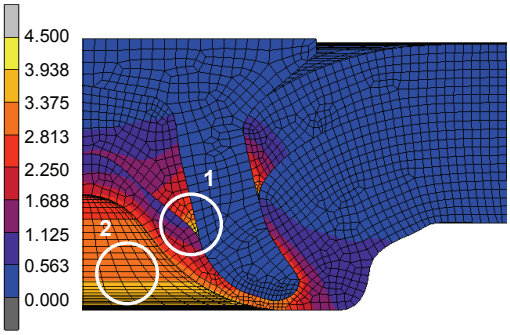

Fig. 7. *The equivalent plastic strain distribution in finished SPR joint.*

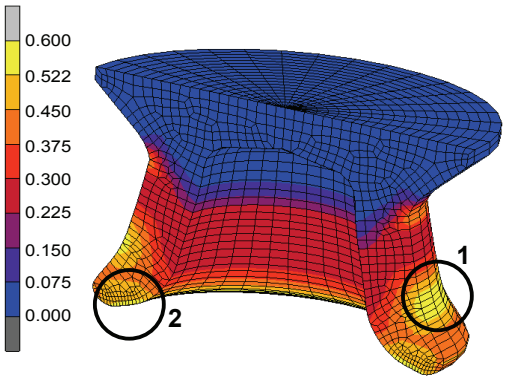

Fig. 8. *The equivalent plastic strain distribution in the rivet, for a finished joint.*

The last stage of the fastener pressing includes restriking in order to flush the rivet head with the upper sheet. Once the punch is moved by s_{max} and right before its retracting, the highest level of the straining of the joint element material may be observed – see figure 9. The tool retraction decreases the stress level in individual joint areas, and this can be assessed by analyzing the residual stress distribution on figure 10.

Such a big material displacement within the joint is accompanied by the rivet and sheet material hardening. During the successive stages of the rivet pushing, the pressure force applied to the punch must increase. The tool retracting means the force decrease and slight de-springing of the joint. The return strains displace the rivet head surface above the upper sheet (area "2") in the considered model by Δx = 0.065 mm, and finally this gives the height of 0.085 relative to the home position of the upper sheet surface of thickness t_{st}. The highest level of stresses can be observed inside the tubular part of rivet (area "1").

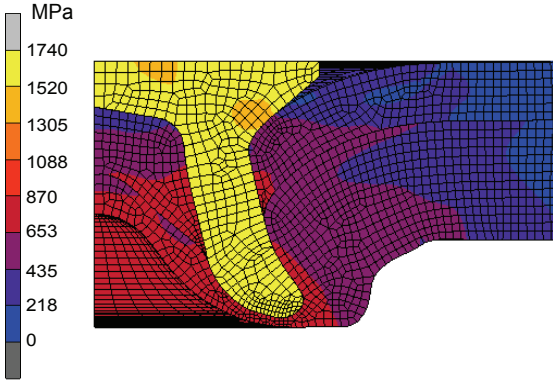

Fig. 9. *The equivalent stress distribution in the joint by HMH during restriking and right before tool retracting.*

The rivet material response during its pressing is its hardening due to corresponding plastic strains. With a diversified rivet material hardening characteristics different behavior of rivet material may be found during the joining process – see figure11b, 12. The higher yield point ratio index S_σ, the higher rivet spread index values are achieved in the joint (figure 12). When using the rivet material of various yield point and of similar hardening curve courses, the fastener gains different forms – see figure 11a. Sooner or later, the rivet begins to upset.

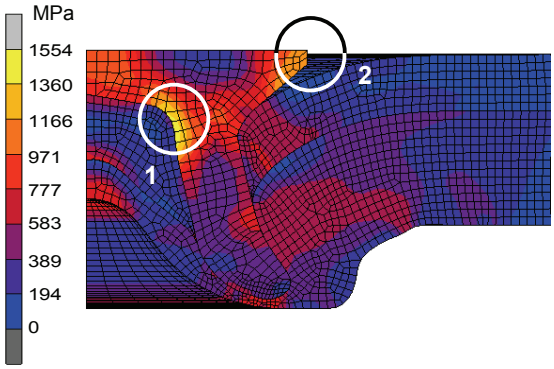

Fig. 10. *The residual stress distribution in the finished joint – the equivalent stress by HMH.*

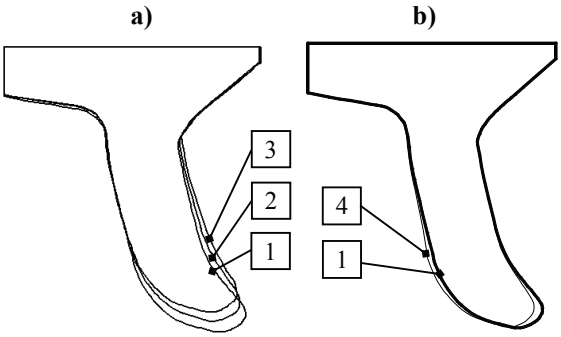

Fig. 11. *The comparison of rivet cross section forms in the finished joint for various rivet material models (see Table 1): a) different values of yield point (rivet material model: 1-3), b) diversified hardening curve course (rivet material model: 1 and 4).*

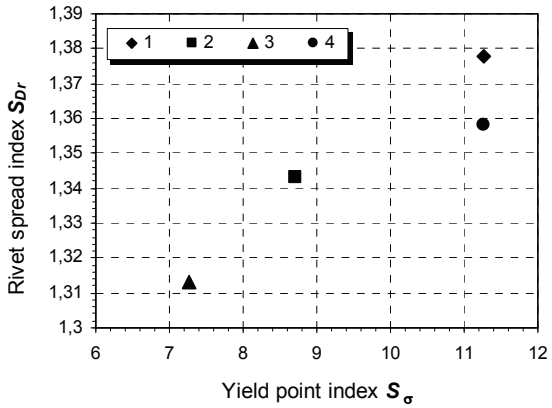

Fig. 12. *The effect of sheet and rivet yield point index to the rivet expansion index in the finished joint (rivet material model 1 - 4).*

When designing the joint, the rivet material may be selected in order to achieve its specific spreading

- see figure 13. The selection of corresponding rivet material features, i.e. plastifying strain and its hardening curve course significantly affects the joint forming process and the final result in form of parameters (for example S_{Dr}), which finally is reflected in the load carrying capacity. When selecting the rivet material for specified combination of joined sheet mechanical properties, besides of the yield point also the material hardening curve course should be accounted for. The difference of yield stresses for upper and lower sheet affects also the joint part behavior when pressing the rivet. However, this requires the separate analysis.

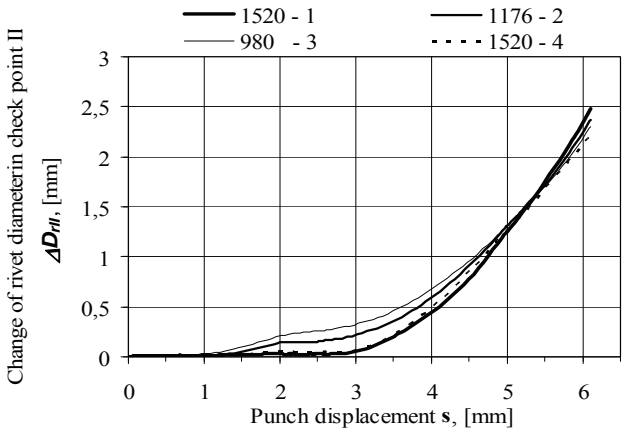

Fig. 13. *The effect of the rivet material on its spreading for a diameter in check point II of rivet model.*

The riveting force courses presented on figure 14 have been determined based on the analysis of three models with different sheet pressing combinations to the front die surface. The force of 200 N caused the indentation of the conical part of die that the sheet plate contacted the die surface. Practically, the pressure force on the blank-holder is within 2000–6500 N. This depends on the sheet material and its thickness.

When no pressing of joined sheets exists, during pressing the fastener the riveting force is offset by s_2 value vs. pressing condition. This because that the pressed rivet has to deform initially the sheets, by pressing them to the die surface. Accordingly, the displacement s_1 is accompanied by the force corresponding to initial sheet bending, relevant to such a tool layout, and the maximum riveting force value differs not much from the force value, achieved when joining the sheets with 200N pressure. Such a joint features high sheet deformations around the fastener and lower adhesion of its elements - lower compactness (figure 15c). Such a joint features lowered rivet head surface in relation to the upper sheet surface by h_2 value, and increased joint height h_1 on the second sheet side, measured in relation to the surfaces created after the sheets are joined. Performing the numerical simulation of the joining process with pressing the blank-holder by 2200N does not significantly affect the riveting force, but increases its maximum value to 16%, when comparing to two other cases. Moreover, the joint created at such pressure parameters features the rivet head protruding slightly the sheet surface by height h_3 = 0.1 mm, as measured from the blank-holder surface – figure 15a.

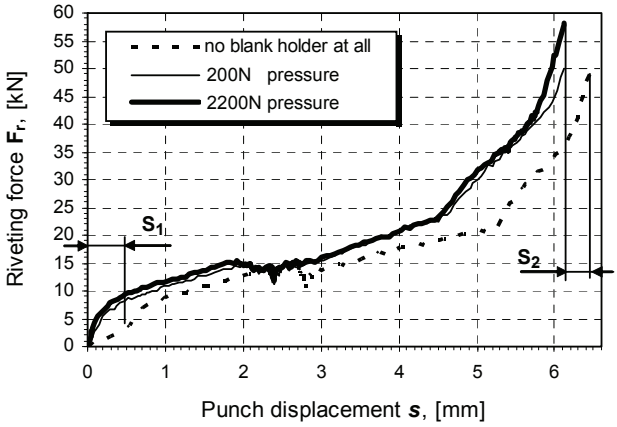

Fig. 14. *The riveting force courses for joining process with different pressure conditions.*

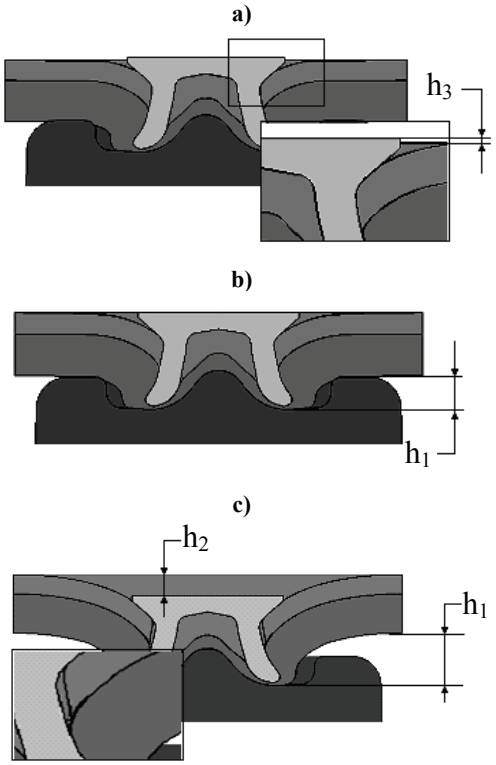

Fig. 15. *The comparison of element deformation for the joint created at different pressure conditions: a) with 2200N pressure, b) zero pressure, c) no sheet pressure at all.*

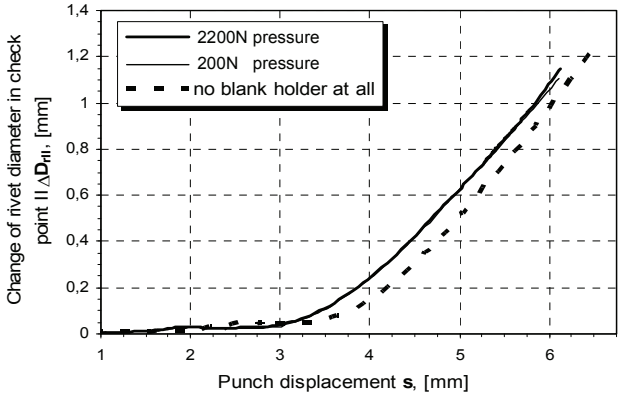

Fig. 16. *The effect of joining pressure conditions on the rivet spreading, for a diameter in check point II of rivet model (rivet material - 1).*

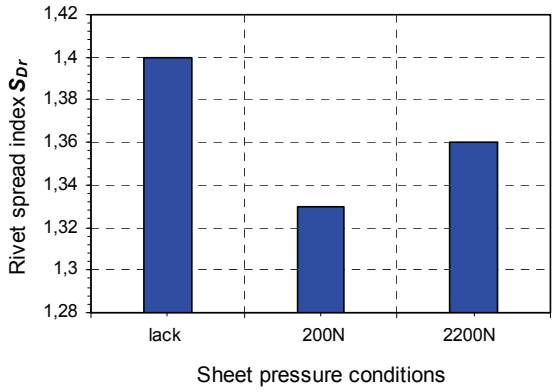

Fig. 17. *The effect of sheet joining pressure conditions on the rivet spreading indicator in the finished joint (rivet material - 1).*

When forming the joint at no pressure at all, the rivet slight longer preserves its form, when comparing to the forming process e.g. with 200N pressure. This affects its spreading when pressing into joined sheets (figure 16). At no pressure at all condition in this joining process, the spreading begins later and lower diameter increase in the tubular pat of rivet check point II may be observed. The pressure force growth occurs to 2200N, gives the effect of the rivet spread index S_{Dr} increase in comparison to zero pressure joining (figure 17). The highest increase may be observed when joining at no pressure at all. However, this results in significant increase of sheet deformation around the joint (figure 15c).

5. CONCLUSIONS

Presented results enable better understanding the effects occurring when creating the SPR joint. The numerical FEM simulation results may be used when designing those modern joints both for other arrangements of joined sheet mechanical properties and the technology used to create them.

Making the joint with no pressure at all has a risk of high deformation of joined elements and its low compactness, and also higher level of the maximum riveting force.

The maximum value of stresses during the joint forming occurs in the rivet right before the tools are retracted. The highest riveting force growth occurs in the restriking stage of the joint forming.

Proper selection of corresponding rivet material features, i.e. its yield point and strain hardening, enables significant changing the sheet joining process and specific finished joint parameters. The maximum rivet immersion (t_2) in the finished joint depends significantly on its yield stress and strain hardening curve under deformations (curves: $\sigma = f(\varepsilon)$). More intensive rivet material hardening increases its hardness, and the rivet deeper penetrates sheet metal being joined. The application of rivet with more flat strain hardening curve causes expansion indicator decrease. In this case, increased upsetting of its tubular part occurs. The higher yield stress, the later rivet expansion and deeper rivet immersion occur.

Summarizing the above considerations, each joint type and its arrangement should be approached individually in order to determine the optimal solution.

REFERENCES

Atzeni, E., Ippolito, R., Settineri, L., 2003, Analysis of the self-piercing riveting process, In: *Proceedings of the Sixth AITEM Conference*, Gaeta, Italy, 281-292.

Atzeni, E., Ippolito, R., Settineri, L., 2004, Numerical and laboratory experiments on self-piercing riveting, In: *Proceedings of the fourth CIRP International Seminar on Intelligent Computation in Manufacturing Engineering, Sorrento*, Italy, 305-309.

Atzeni, E., Ippolito, R., Settineri, L., 2009, Experimental and numerical appraisal of self-piercing riveting, *CIRP Annals - Manufacturing Technology*, 58, 17-20.

Barnes, T.A., Pashby, I.R., 2000, Joining techniques for aluminium spaceframes used in automobiles Part II – adhesive bonding and mechanical fasteners, *Journal of Materials Processing Technology*, 99, 72-79.

Bouchard, P.O., Laurent, T., Tollier, L., 2009, Numerical modeling of self-pierce riveting–From riveting process modeling down to structural analysis, *Journal of Materials Processing Technology*, 202, 290-300.

Cacko, R., Czyżewski, P., 2007, Verification of numerical modelling of the SPR joint by experimentul stack-up, *Computer Methods in Materials Science*, 7/1, 124-129.

Cacko, R., Czyżewski, P., and Kocańda, A., 2004, Initial optimization of self-piercing riveting rocess by means of FEM, *Steel Grips, 2*, 307-310.

Cai, W., Wang and Wu Yang P.C., 2005, Assembly dimensional prediction for self-piercing riveted aluminum panels, *In-*

ternational Journal of Machine Tools & Manufacture, 45, 695-704.

Di Lorenzo, G., Landolfo, R., 2004, Shear experimental response of new connecting systems for cold-formed structures, *Journal of Constructional Steel Research*, 60, 561-579.

Gårdstam, J., 2006, *Simulation of mechanical joining for automotive applications*, Licentiate Thesis from Royal Institute of Technology, Department of Mechanics, SE-100 44 Stockholm, Sweden, 1-17.

Hahn, O., Dölle, N., 2001, *Numerische Simulation des Fügeprozesses beim Stanznieten mit Halbhohlniet von duktilen Blechwerkstoffen*, Universität Paderborn, LWF Schriftreihe 48, Shaker Verlag, Aachen.

MSC.Marc Volume A: Theory and user information. Version 2005.

Mucha J., 2007, History of the riveted joint technique (Self Piercing Riveting – SPR), *Mechanik*, 5-6, 454-460.

Mucha, J., 2009a, Numeric study of the phenomena occurring in the self piercing riveting process, *Mechanik*, 4, 286-291.

Mucha J., 2009b, Some aspects of designing process self piercing riveting, Polish Academy of Sciences Poznan Division, *Archives of Mechanical Technology and Automation*, 29/4, 91-101.

Porcaro, R., Hanssen, A.G., Langseth, M., Aalberg, A., 2006, Self-piercing riveting process: An experimental and numerical investigation, *Journal of Materials Processing Technology*, 171 10-20.

NUMERYCZNA ANALIZA ODKSZTAŁCANIA SIĘ NITA PODCZAS ŁĄCZENIA BLACH ALUMINIOWYCH ZA POMOCĄ NITOWANIA BEZOTWOROWEGO

Streszczenie

Nitowanie bezotworowe jest nowoczesną i nową metodą łączenia, stosowaną w przemyśle samochodowym do łączenia blach aluminiowych. Jest to proces kształtowania na zimno, w którym wtłaczany nit rurkowy przebija górną blachę rozszerzając się przy tym wciska w dolną tak, że powstaje nierozłączne połączenie.

Praca zawiera symulację numeryczną procesu nitowania za pomocą metody elementów skończonych w programie MSC.Marc. Analizę nitowania wykonano dla łączonych blach aluminiowych. Autor na podstawie otrzymanych wyników z obliczeń numerycznych podjął się próby wyjaśnienia zjawisk zachodzących w tym procesie. Wykonano analizę porównawczą w obszarze eksperymentu numerycznego, wpływu zmiany różnych parametrów nitowania na efekt odkształcania się nita.

Received: January 1, 2010
Received in a revised form: March 8, 2010
Accepted: May 19, 2010